Available online at www.sciencedirect.com

SCIENCE DIRECT®

Marine Chemistry 96 (2005) 257–271

MARINE CHEMISTRY

www.elsevier.com/locate/marchem

Major deviations of iron complexation during 22 days of a mesoscale iron enrichment in the open Southern Ocean

Marie Boye[a,c,*], Jun Nishioka[b], Peter L. Croot[a], Patrick Laan[a], Klaas R. Timmermans[a], Hein J.W. de Baar[a]

[a]*Royal Netherlands Institute for Sea Research, Postbus 59, 1790 AB Den Burg-Texel, The Netherlands*
[b]*Central Research Institute of Electric Power Industry, Abiko, Chiba 270-1194, Japan*
[c]*Currently at Laboratoire des Sciences de l'Environnement Marin (LEMAR), CNRS UMR6539/IUEM, Technopôle de Brest-Iroise, Place Nicolas Copernic, 29 280 Plouzané, France*

Received 20 November 2003; accepted 14 February 2005
Available online 24 May 2005

Abstract

The speciation of strongly chelated iron during the 22-day course of an iron enrichment experiment in the Atlantic sector of the Southern Ocean deviates strongly from ambient natural waters. Three iron additions (ferrous sulfate solution) were conducted, resulting in elevated dissolved iron concentrations (Nishioka, J., Takeda, S., de Baar, H.J.W., Croot, P.L., Boye, M., Laan, P., Timmermans, K.R., in press. Changes in the concentration of iron in different size fractions during an iron enrichment experiment in the open Southern Ocean. *Marine Chemistry*.) and significant Fe(II) levels (Croot, P.L., Laan, P., Nishioka, J., Strass, V., Cisewski, B., Boye, M., Timmermans, K.R., Bellerby, R.G., Goldson, L., Nightingale, P., de Baar, H.J.W., in press. Spatial and Temporal distribution of Fe(II) and H_2O_2 during EisenEx, an open ocean mescoscale iron enrichment. *Marine Chemistry*.). Repeated vertical profiles for dissolved (filtrate <0.2 μm) Fe(III)-binding ligands indicated a production of chelators in the upper water column induced by iron fertilizations. Abiotic processes (chemical reactions) and an inductive biologically mediated mechanism were the likely sources of the dissolved ligands which existed either as inorganic amorphous phases and/or as strong organic chelators. Discrete analysis on ultra-filtered samples (<200 kDa) suggested that the produced ligands would be principally colloidal in size (>200 kDa–<0.2 μm), as opposed to the soluble fraction (<200 kDa) which dominated prior to the iron infusions. Yet these colloidal ligands would exist in a more transient nature than soluble ligands which may have a longer residence time. The production of dissolved Fe-chelators was generally smaller than the overall increase in dissolved iron in the surface infused mixed layer, leaving a fraction (about 13–40%) of dissolved Fe not bound by these dissolved Fe-chelators. It is suggested that this fraction would be inorganic colloids. The unexpected persistence of such high inorganic colloids concentrations above inorganic Fe-solubility limits illustrates the peculiar features of the chemical iron cycling in these waters. Obviously, the artificial about hundred-fold increase of overall Fe levels by addition of dissolved inorganic Fe(II) ions yields a major disruption of the natural physical–chemical abundances and reactivity of Fe in seawater.

* Corresponding author. Laboratoire des Sciences de l'Environnement Marin (LEMAR), CNRS UMR6539/IUEM, Technopole de Brest Iroise, Place Nicolas Copernic, 29 280 Plouzané, France. Tel.: +33 2 98 49 86 51; fax: +33 2 98 49 86 45.
E-mail address: marie.boye@univ-brest.fr (M. Boye).

0304-4203/$ - see front matter
doi:10.1016/j.marchem.2005.02.002

Hence the ensuing responses of the plankton ecosystem, while in itself significant, are not necessarily representative for a natural enrichment, for example by dry or wet deposition of aeolian dust.

Ultimately, the temporal changes of the Fe(III)-binding ligand and iron concentrations were dominated by the mixing events that occurred during EISENEX, with storms leading to more than an order of magnitude dilution of the dissolved ligands and iron concentrations. This had strongest impact on the colloidal size class (>200 kDa–<0.2 μm) where a dramatic decrease of both the colloidal ligand and the colloidal iron levels (Nishioka, J., Takeda, S., de Baar, H.J.W., Croot, P.L., Boye, M., Laan, P., Timmermans, K.R., in press. Changes in the concentration of iron in different size fractions during an iron enrichment experiment in the open Southern Ocean. *Marine Chemistry.*) was observed.

Keywords: Southern Ocean; Iron enrichment experiment; Organic speciation

1. Introduction

The organic complexation of iron is a central factor in oceanic iron cycling, as the organic Fe-binding ligand acts to retain iron in oceanic waters, increasing the otherwise very low (~0.1 nM) iron solubility in oxic oceanic waters (Kuma et al., 1996; Wu et al., 2001). The overall excess of organic ligand over dissolved iron observed in the world's oceans (*Pacific*, Rue and Bruland, 1995; *Southern Ocean*, Boye et al., 2001; Croot et al., 2004; *Atlantic*, Gledhill and van den Berg, 1994; Witter and Luther, 1998; Powell and Donat, 2001; *Mediterranean Sea*, Van den Berg, 1995; *Arabian Sea*, Witter et al., 2000) indeed suggests that iron removal from seawater by scavenging is largely slowed down once the overall dissolved Fe concentration comes below the ligand concentration. Though compelling studies demonstrated the impact of the organic complexation on the oceanic geochemistry of iron, the oceanic cycling of the organic ligands is not completely understood yet. For example, the sources of the organic ligands have not been clearly identified, while field observations (Van den Berg, 1995; Rue and Bruland, 1997; Boye et al., 2001; Croot et al., 2004) and culture experiments (Reid and Butler, 1991; Boye and van den Berg, 2000) have suggested biological sources of the ligand (by phytoplankton and/or bacteria). Furthermore, the chemical structure and speciation of the dissolved ligand(s) still need to be further revealed. This is important towards understanding the dynamics of iron in oceanic waters, hence the selective bio-availability of different chemical forms of iron to the micro-organisms. For instance, only a few works have examined the functionality and structure of various marine siderophores and their degradation products (Barbeau et al., 2001; Reid et al., 1993). In addition, the chemical speciation of the organic Fe-ligands, described by the ligand concentration and the Fe-ligand complexing stability, indicated so far the presence of maximum two chemical classes of dissolved organic Fe-chelators, such as detected in the Pacific Ocean (Rue and Bruland, 1995, 1997). Recent evidences showed that the speciation of the ligand(s) has also to be interpreted according to the size-spectrum of the operationally defined (<0.4 or 0.2-μm filtrate) so-called 'dissolved' fraction. Two size classes of organic ligands have indeed been identified in the dissolved waters of the north Atlantic and north Pacific Oceans, one class found to be soluble (<0.02 μm) while the other class was in the colloidal size range (0.02 to 0.4 μm) (Wu et al., 2001). The two size classes of ligand ensure the organic complexation of iron in the colloidal and the soluble fractions, each with different chemical reactivities in the water column, hence conceivably different bio-availability (Wu et al., 2001).

Mesoscale iron fertilizations conducted in the High Nutrient Low Chlorophyll (HNLC) regions of the global ocean including the Equatorial Pacific (Martin et al., 1994; Coale et al., 1996), the Southern Ocean (Boyd and Law, 2001; Coale et al., 2004) and the North Pacific (Tsuda et al., 2003; Boyd et al., 2004) have demonstrated the limiting role of iron on phytoplankton growth in these areas. These studies, based on a major perturbation of natural cycling by adding large amounts of iron, have also revealed some unique information about the dynamical processes affecting iron cycling (Rue and Bruland, 1997; Coale et al., 1996; Gordon et al., 1998; Bowie et al., 2001;

Croot et al., 2001; Wells, 2003), although uncertainties still remain in our understanding of the biogeochemical cycling of iron in the ocean (Hunter et al., 2001).

In an effort to further understand the oceanic cycling of the ligands, hence, the iron biogeochemical dynamics, the present work examines the changes in the complexation of iron during a 22-day mesoscale iron enrichment experiment in the Atlantic sector of the Southern Ocean (EisenEx). Here, the changes in the ligands in both the 'dissolved' fraction (<0.2-μm filtrate), and the smaller 'soluble' size fraction (<200-kDa ultrafiltrate) of discrete samples, are presented. Combination of this work with studies of the Fe-redox speciation (Croot et al., in press) and the distribution in size of dissolved Fe (Nishioka et al., in press) aims at new insights into the biogeochemical cycling of iron.

2. Sampling and methods

2.1. Sampling

Samples were collected in the Atlantic sector of the Southern Ocean in late austral spring (November 6–29, 2000) on board the Research Vessel *Polarstern* (ANTXVIII/2 cruise) during the mesoscale iron enrichment experiment EisenEx (Gervais et al., 2002). Three iron infusions (780 kg Fe(II) each, in acidic ferrous sulfate $FeSO_4$ solution in seawater) were made at days zero, 7/8 and 16 in a dual labeled (SF_6 and ^3He) mesoscale eddy at about 30 m depth (Bakker et al., in press). Three storm tracks crossed the patch area at days 5, 13 and 17 during the time of survey (Bozec et al., in press). A timeline of sampled stations, Fe-infusions and major storm events is given in Table 1. Due to the storm events, the original Fe/SF_6/^3He enriched patch of almost 50 km^2 had at day 22 been diluted and expanded to almost 1000-km^2 surface area (Bakker et al., in press). Due to the highly erratic nature of this storm dilution and mixing, also with underlying waters, it has thus far proven difficult to arrive at a mass balance of the initial additions of tracers SF_6 and ^3He, where apart from lateral and vertical mixing a loss term due to air/sea gas exchange is also to be taken into account (Bakker et al., in press; Goldson, 2004).

Vertical sampling was performed at stations inside (as defined by the highest observed SF_6 concentrations) and outside (with only pre-infusion background SF_6 concentrations) the patch. The initial distributions of the ligands and the iron concentrations were obtained by averaging and combining four out-patch stations sampled before and during the Fe-experiment between Nov 2 and 25 (St. 007, St. 009, St. 048 and St. 091). Details on the ambient distribution of the ligands in the different size classes are given elsewhere (Boye et al., in prep.). The vertical distributions of the organic ligands and iron inside the patch were studied between 20 and 100 m depth, encompassing the depth of the Fe-release (~30 m) and the mixed layer depth which was typically less than 40 m during the first 2 weeks but increasing to greater than 80 m over the final 2 weeks of the experiment (Gervais et al., 2002; Bakker et al., in press).

Table 1
Timeline of iron organic complexation sampling in the upper 100 m, of the three iron release events and the three storms during EisenEx

Station number	Date	Time after 1st Fe-release (day)	Event
	Nov 7–8		First Fe-release
St. 011	Nov 9	1	
St. 014	Nov 10	2	
St. 038	Nov 11	3	
St. 041	Nov 12	4	
	Nov 12–13		First storm
St. 045	Nov 15	7	
	Nov 15–16		Second Fe-release
St. 046	Nov 16	8	
St. 049	Nov 18	10	
St. 061	Nov 20	12	
	Nov 20–22		Second storm
St. 088	Nov 24	16	
	Nov 24		Third Fe-release
	Nov 26		Third storm
St. 092	Nov 27	19	
St. 107	Nov 29	21	

Seawater samples were collected at depth using acid-cleaned Teflon coated Go-Flo samplers suspended on a Kevlar wire (Croot et al., in press). Filtered samples (<0.2 μm; Sartorius Sartobran filter capsule) were collected into acid-cleaned 500-ml NALGENE polycarbonate bottles. Additional filtrate (<0.2 μm) samples were immediately size fractionated by a clean inline ultrafiltration system using a 200-kDa (~0.03 μm) polyethylene hollow-fiber ultrafilter unit (STERAPORE) at onboard laminar flow clean air hood (Nishioka et al., in press). The smaller fraction (<200 kDa) was collected in acid cleaned

low-density polyethylene or/and polycarbonate bottles. Operational definitions were taken as "dissolved" being the filtrate <0.2 μm, soluble" being the ultrafiltrate <200 kDa. As pointed out previously (Nishioka et al., 2001), the soluble Fe fraction may include some very small colloids, since the potential existence of 1- to 1000-Da size colloids has been reported in seawater (Wells et al., 1998).

The samples were analyzed on shipboard directly after collection of the samples or within 1–2 days of the collection (between the time of collection and analysis on-board, the samples were left in a refrigerator at ~4 °C). Ultrafiltration, sample treatments and measurements were carried out in a clean container under laminar flow hood with High Efficiency Particle Arrestance (HEPA) clean filtered air.

2.2. Analytical procedures

2.2.1. Iron determination

The iron concentrations (dissolved and soluble fractions) were determined as Fe(III)-species with an automatic flow injection analytical system (Kimoto Electric, Ltd.) using concentration onto an 8-hydroxyquinoline chelating column, after acidification at pH 3.2 and chemiluminescence detection (Obata et al., 1993; Nishioka et al., in press). The analytical method and the results of the temporal changes of the Fe concentrations in the different size fractions during the EisenEx experiment are discussed in full detail in Nishioka et al. (in press). Dissolved and soluble iron concentrations were used to estimate the organic speciation in the dissolved and soluble size fractions respectively.

2.2.2. Fe-complexation determination

The complexation of iron was determined by complexing capacity titrations in the dissolved (<0.2 μm) filtrate and for discrete samples in the soluble (<200 kDa) filtrate, using cathodic stripping voltammetry (CSV) with ligand competition against 2-(2-thiazolylazo)-*p*-cresol (TAC) (adapted from Croot and Johansson, 2000).

The analytical procedure is similar to that described in Boye et al., 2001, with the exception that the competitive ligand TAC was used instead of 1-nitroso-2-naphtol (NN). Titrations were carried out at pH 8.1 using borate buffer (H_3BO_3, BDH) with 10 μM of TAC. The borate stock solution (1 M boric acid/0.3 M ammonia) was cleaned by equilibration with TAC (40 μM), followed by extraction using a Sep-Pak C18 cartridge (activated with methanol) and was used to a final concentration of 5 mM. A methanolic solution of 2-(2-thiazolylazo)-*p*-cresol (TAC) ($C_{10}H_8OH.N_3.S$, Aldrich) was prepared containing 0.02 M TAC using 3-times quartz-distilled methanol and was used to a final concentration of 10 μM. Samples were titrated with iron (using a stock solution of 10^{-6} M Fe^{III} prepared in 0.01 M quartz-distilled hydrochloric acid) which was added in 11 increments on the order of 0.25 nM to 1 nM Fe ranging between 0 and 8 nM. The Teflon vials containing the sample and the reagents (Fe^{III} standard, borate buffer and TAC solution) were left for equilibration for 12–15 h, at room temperature in a laminar flow hood. Distinct series of Teflon vials were used for expected "high-Fe" and "low-Fe" levels.

Two identical voltammeters, consisting of a mercury drop electrode (model VA663 from Metrohm, Switzerland) connected to a voltammeter (μAutolab from Eco Chemie, Netherlands) were used simultaneously to increase the sample throughput. The reference electrode was a double-junction, Ag/AgCl, 3 M KCl, with a salt bridge filled with 3 M KCl and the counter electrode was glassy carbon.

After purging each solution with O_2-free nitrogen for 200 s, the measurements were made using an adsorption time of 200 to 400 s at an adsorption potential of −0.4 V, followed by a 10-s quiescence period after which the potential was scanned from −0.4 to −0.9 V using the fast linear sweep waveform (10.1 V s^{-1} potent1ial 1.98 mV) (Croot and Johansson, 2000). Using this procedure, the detection limit of labile Fe(III) concentrations (three time the standard deviation of five measurements) with borate buffer (5 mM) and TAC solution (10 μM) added to a sample containing low dissolved-[Fe] (~0.15 nM) was 30 pM.

The ligand concentrations ([*L*]) and conditional stability constants

$$\left(K'_{\mathrm{FeL}} = \frac{[\mathrm{FeL}]}{[\mathrm{Fe}^{3+}][L']}\right) \quad (1)$$

were calculated by linear least-squares regression of the data fitted to the following equation (Van den

Berg and Kramer, 1979; Ruzic, 1982; Van den Berg, 1982):

$$\frac{[\mathrm{Fe_{labile}}]}{[\mathrm{FeL}]} = \frac{[\mathrm{Fe_{labile}}]}{[L]} + \frac{(\alpha_{\mathrm{Fe'}} + \alpha_{\mathrm{FeTAC_2}})}{[L]K'_{\mathrm{FeL}}}. \quad (2)$$

The inorganic side reaction coefficient for iron was taken as $\log\alpha_{\mathrm{Fe'}}=10$ (Hudson et al., 1992), and for $FeTAC_2$ as $\log a_{\mathrm{FeTAC2}}=12.4$ (using $\log\beta'_{\mathrm{FeTAC2}}=22.4$; Croot and Johansson, 2000, and [TAC]=10 μM), providing a detection window (Van den Berg and Donat, 1992) of $10^{11.4}$ to $10^{13.4}$. The standard deviations of $[L]$ and $\log K'$ (stdv) are calculated from linear least-squares regression of the titration curves fitted for a single ligand (Boye et al., 2001). The relative standard deviation of repeated (3×) determinations of the ligand concentration was better than 5% and better than 1% for the conditional stability constant (on samples containing low and high dissolved iron concentration). The TAC-labile Fe concentrations (forming $FeTAC_2$ complexes during the titration and detected at the zero addition of standard Fe) recorded in the natural waters and in the course of the experiment ranged between 0.025 nM and 1.8 nM and were lower than the dissolved Fe levels (0.04–5.5 nM). Both parameters were linearly correlated according to:

$$[\mathrm{TAC-labile\ Fe}] = 0.32[\mathrm{dissolved-Fe}] + 0.02 \quad (r^2 = 0.94, n = 62) \quad (3)$$

Viewed at the lowest concentration ranges, this equation strongly suggested that Fe contamination from reagents was minor in the titrations, while in itself it does not prove that the reagents Fe-blank of the CSV-measurement was negligible. The speciation of iron (the concentrations of Fe(III) bound to the detected ligands [FeL], and not bound to these ligands [Fe′]) were calculated at the thermodynamic equilibrium (Boye et al., 2001).

3. Results

3.1. The trends of iron

Iron additions (first and second releases) resulted in an increase by about 20–58 times of the dissolved Fe (DFe) concentrations in the fertilized mixed layer up to 5.5 nM compared to the pre-release concentration which was as low as 40 pM (Nishioka et al., in press; Fig. 1). The high concentrations of DFe were kept in the mixed layer for about 4 days after the first and the second Fe-releases, and ultimately dropped after each storm event (Nishioka et al., in press; Fig. 1). The difference between the dissolved-fraction and the soluble fraction was used as an indirect estimation of the Fe concentration in the small colloidal fraction (e.g., >200 kDa–<0.2 μm; Nishioka et al., in press). The inorganic iron additions induced a shift in the proportions of each size fraction toward the predominance of the colloidal fraction in the fertilized waters (~76% vs. DFe, as compared to ~35% in the natural waters; Nishioka et al., in press). The colloidal iron was also the fraction which was eliminated from the surface mixed layer more easily than the soluble fraction after the storm events (Nishioka et al., in press).

3.2. The dynamics of the dissolved ligands

The vertical distribution of the dissolved ligand was modified after a Fe-infusion (Fig. 1). Upon the first and the second Fe-infusions, much higher concentrations of dissolved ligand were observed in the upper water column compared to greater depths (Fig. 1). This is the opposite of the slight increase of the ligand concentration with depth as observed in the ambient natural conditions (Fig. 1). Yet after each of the three storm events, the vertical distribution of the dissolved ligand returned to the pre-infusion conditions (Fig. 1). The concentrations of the dissolved ligands also changed after Fe-additions and storm events (Table 2, Fig. 1). Ligand concentrations increased rapidly (~4–12 h) and almost continuously or were kept at high value (for 4 days) in the upper water layer after the first and the second infusions. In contrast after each storm the ligand concentrations had dropped to or near ambient concentrations.

Averaged ligands concentrations were calculated within (e.g., the upper 40 m until Day 7 and the upper 60 m from Day 7 to Day 21) and below (60 to 100 m until Day 7 and 80 to 100 m from Day 7 to Day 21) the surface mixed layer depth (Fig. 2). Only few hours after the first infusion (~12 h), the dissolved averaged

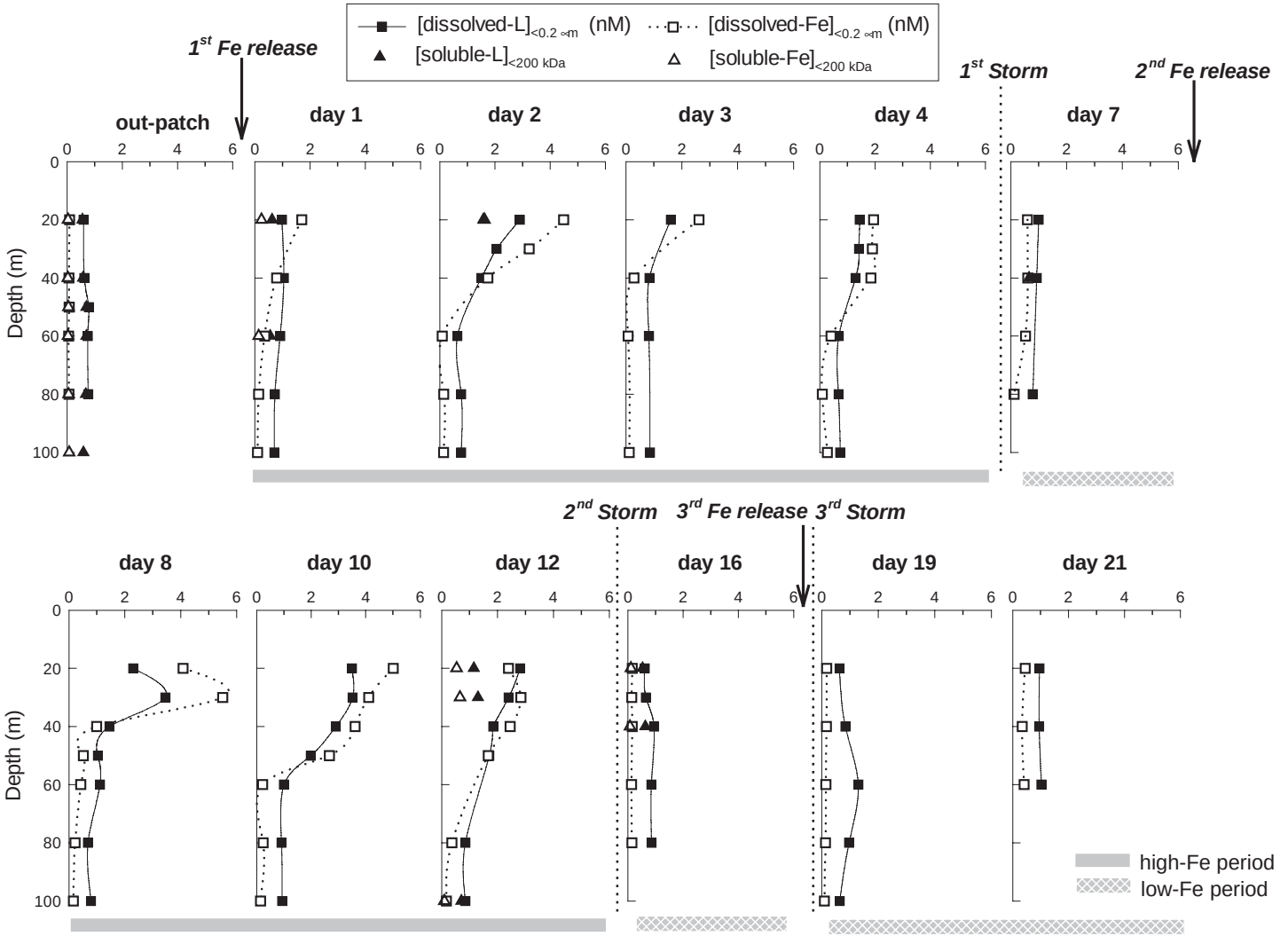

Fig. 1. The time course of the concentrations along vertical distributions of dissolved (<0.2 μm) Fe (□) and soluble (<200 kDa) Fe (△), and of dissolved (<0.2 μm) Fe(III)-binding ligand (■) and soluble (<200 kDa) Fe(III)-binding ligand (▲) during EisenEx. The events of Fe-infusion and storms are indicated by arrows and dotted vertical lines respectively (actual dates listed in Table 1). The high and low dissolved iron concentration periods in the surface mixed layer are also indicated by horizontal grey and hatched bars, respectively.

Table 2
The dissolved (<0.2 μm) iron ([Fe], Nishioka et al., in press), dissolved Fe(III)-binding ligand concentrations ([L]) and their conditional stability constants with dissolved iron (logK') from the vertical casts during the EisenEx experiment

Day after the 1st Fe-release (Station number)	Depth (m)	[Fe] (nM)	[L] (nM)	Stdv [L] (nM)	LogK'	Stdv logK'
OUT-patch	20	0.09	0.60	0.04	21.82	0.15
	40	0.07	0.63	0.12	22.21	0.73
	50	0.08	0.79	0.07	22.04	0.33
	60	0.06	0.75	0.03	22.01	0.19
	80	0.07	0.77	0.13	21.66	0.19
	100	NA	NA	NA	NA	NA
Day 1 (st. 011)	*20*	1.7	0.98	0.04	22.63	0.55
	40	0.79	1.05	0.06	22.87	0.83
	60	0.36	0.92	0.09	22.60	0.78
	80	0.14	0.73	0.10	21.64	0.30
	100	0.1	0.71	0.03	22.16	0.20
Day 2 (st. 014)	*20*	4.49	2.90	0.08	ND	ND
	30	3.24	2.06	0.07	22.25	0.30
	40	1.74	1.51	0.27	21.29	0.14
	60	0.09	0.64	0.08	22.04	0.42
	80	0.15	0.78	0.05	22.55	0.55
	100	0.14	0.78	0.05	22.12	0.22
Day 3 (st. 038)	*20*	2.62	1.61	0.07	22.34	0.41
	40	0.29	0.84	0.08	21.58	0.14
	60	0.08	0.82	0.09	21.35	0.08
	100	0.12	0.86	0.14	21.43	0.14
Day 4 (st. 041)	*20*	1.95	1.45	0.08	21.98	0.25
	30	1.91	1.42	0.09	22.09	0.34
	40	1.85	1.30	0.05	22.18	0.26
	60	0.41	0.69	0.04	22.10	0.31
	80	0.09	0.68	0.14	21.09	0.05
	100	0.28	0.74	0.07	22.27	0.52
Day 7 (st. 045)	20	0.6	1.00	0.02	22.44	0.24
	40	0.61	0.93	0.08	22.44	0.62
	80	0.12	0.79	0.17	21.05	0.04
Day 8 (st. 046)	*20*	4.08	2.88	0.09	ND	ND
	30	5.5	3.45	0.10	ND	ND
	40	0.99	1.45	0.06	22.13	0.24
	50	0.52	1.04	0.08	22.64	0.70
	60	0.42	1.11	0.03	22.07	0.25
	80	0.22	0.68	0.08	21.86	0.28
	100	0.16	0.79	0.11	21.54	0.17
Day 10 (st. 049)	*20*	5.01	3.49	0.10	ND	ND
	30	4.11	3.52	0.09	22.25	0.24
	40	3.61	2.90	0.13	21.90	0.19
	50	2.67	1.99	0.02	23.00	0.39
	60	0.22	1.00	0.06	22.15	0.28
	80	0.24	0.91	0.07	22.80	0.80
	100	0.14	0.93	0.06	21.92	0.19
Day 12 (st. 061)	*20*	2.39	2.81	0.08	22.10	0.17
	30	2.84	2.40	0.07	22.78	0.55
	40	2.45	1.85	0.07	22.32	0.36
	50	1.67	1.71	0.04	22.42	0.26
	80	0.37	0.85	0.09	22.10	0.40
	100	0.17	0.85	0.08	21.52	0.11
Day 16 (st. 088)	20	0.16	0.61	0.06	22.08	0.39
	30	0.14	0.65	0.04	23.81	1.66
	40	0.16	0.95	0.05	22.40	0.37
	60	0.13	0.85	0.07	21.72	0.17
	80	0.15	0.86	0.11	21.47	0.13
Day 19 (st. 092)	20	0.18	0.63	0.07	21.32	0.08
	40	0.17	0.84	0.02	21.96	0.09
	60	0.15	1.30	0.04	21.80	0.07
	80	0.14	0.97	0.06	21.59	0.09
	100	0.1	0.64	0.05	21.84	0.22
Day 21 (st.107)	20	0.45	0.96	0.05	22.20	0.30
	40	0.34	0.95	0.04	22.41	0.37
	60	0.41	1.03	0.03	22.09	0.17

Both for the ligand concentration and for the stability constant the standard deviation estimate is also listed (see the text for the standard deviation (stdv) calculations).
NA denotes Not Analyzed. ND denotes Not Determined (e.g., no mathematical resolution).
Depths in italic indicate high [DFe] (>1.7 nM).
Underlined depths indicate straight titrations in the dissolved fraction.

ligand concentration increased in the surface mixed layer by a factor 1.5 compared to out-patch concentrations. Next a 2- to 3-fold increase (relative to out-patch) was observed during the following three days (Fig. 2). The first storm event was at the end of Day 4, and the concentrations had dropped by Day 7, but still were higher by a factor 1.4 than the out-patch concentrations. After the second Fe-infusion (on Days 7–8), the ligand concentrations again increased very rapidly within the mixed layer already after ~4 h following the infusion. Moreover, this increase was in higher proportion than after the first infusion, up to a 4-fold increase. A second storm crossed the patch-area at the end of Day 12 and stayed on the area until Day 15. After this storm, the ligand concentrations within the mixed layer once again had dropped to almost ambient natural values, i.e., [L] was about 0.7 nM. A third Fe-infusion was conducted starting at the end of Day 16, but before a station was sampled a third (and weaker) storm crossed the area (at the end of Day 18). The dissolved ligand concentrations measured in the mixed layer after these two events (on Days 19, 21) still showed higher concentrations by about 1.4-fold

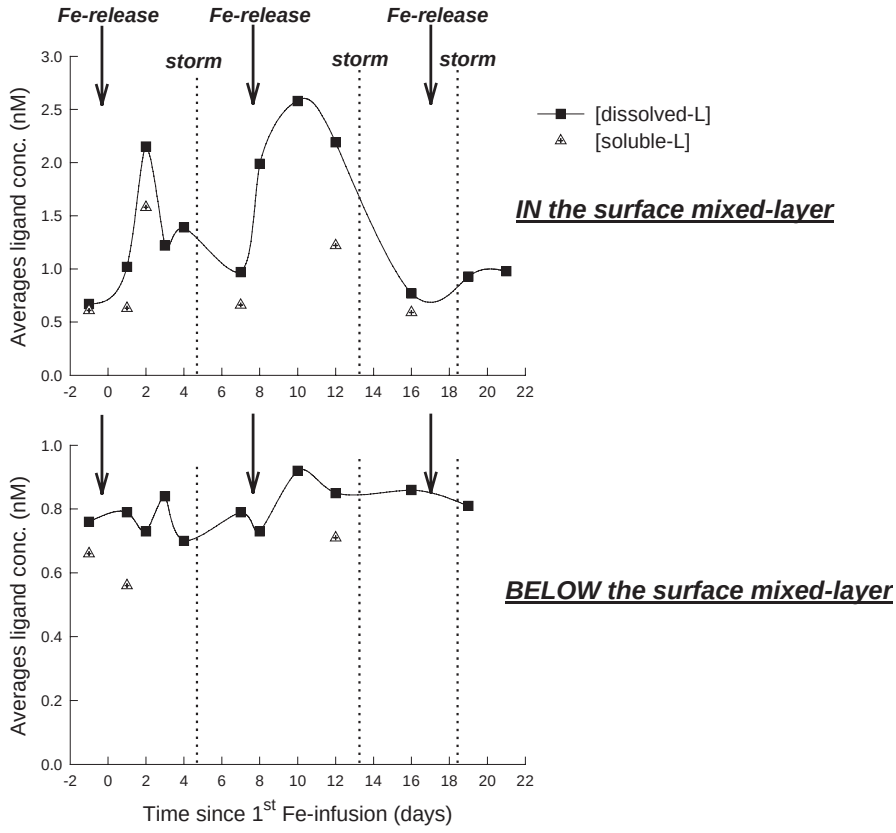

Fig. 2. The temporal changes in the averaged dissolved and soluble ligands concentrations within the surface mixed layer (upper graph) and in the deeper waters below the mixed layer (lower graph) during the course of the enrichments experiment.

compared to the initial conditions. However, the increase was small relative to pre-3rd infusion levels, an increase from 0.8 nM on Day 16 to about 0.9–1 nM on Days 19, 21.

In the deeper waters below the mixed layer, the mean ligand concentration was overall in the same range as the out-patch concentrations (~0.76 nM, Fig. 2). Slight increases in [L] were however observed on Day 3 (from initial 0.76 to 0.84 nM) and on Day 10 (up to 0.92 nM) (Fig. 2) and generally slightly higher values were observed in deep waters during the last week of the experiment (from Day 12 until Day 19, Fig. 2) but this enhancement was modest by a factor 1.1 only. A lag-period of 1–2 days between the start of the increase of ligand concentration in the surface mixed layer and the (slight) increase recorded in deeper waters was observed after the first infusion as well as after the second infusion (Fig. 2).

3.3. The size-distribution of the dissolved ligands

Based on discrete determinations of the soluble ligand concentrations (Table 3), two major features emerged:

i) Soluble ligands were produced within the mixed layer after the first and second Fe-infusions (Figs. 1 and 2). However, a dramatic increase up to 35-fold of the difference between dissolved and soluble ligands concentrations was observed, much more dramatic than the increasing concentrations by 2- to 3-fold for soluble ligand, all relative to their respective out-patch levels (Table 3). The difference between dissolved and soluble ligand concentrations is presumably due to colloidal ligands (e.g., >200 kDa–<0.2 μm). One iron addition effect would thus be to cause a higher production of colloidal ligands compared to soluble ligands.

Table 3
Soluble (<200 kDa) iron concentrations ($[Fe]_{soluble}$) from the vertical casts (Nishioka et al., in press)

Day after the 1st Fe-fertilisation (Station number)	Depth (m)	$[Fe]_{soluble}$ (nM)	$[L]_{soluble}$ (nM)	Stdv $[L]_{soluble}$ (nM)	$\log K'_{soluble}$	Stdv $\log K'_{soluble}$	$[L]_{dissolved} - [L]_{soluble}$ (nM)	$[L]_{soluble}/[L]_{dissolved}$ (%)
OUT-patch	20	0.04	0.56	0.08	22.39	0.72	b.d.	94
	40	0.03	0.58	0.06	21.99	0.37	b.d.	92
	50	0.05	0.70	0.05	21.61	0.11	b.d.	89
	60	0.04	0.70	0.11	21.55	0.19	b.d.	94
	80	0.06	0.68	0.05	21.64	0.14	b.d.	88
	100	0.08	0.59	0.10	21.44	0.15	ND	ND
Day 1 (st. 011)	*20*	0.24	0.63	0.04	21.86	0.17	0.35	64
	60	0.14	0.56	0.12	21.41	0.17	0.36	61
Day 2 (st. 014)	20	1.62	1.58	0.04	22.76	0.46	1.32	54
Day 7 (st. 045)	40	0.16	0.66	0.05	21.75	0.17	0.27	71
Day 12 (st. 061)	*20*	0.54	1.15	0.05	21.93	0.15	1.65	41
	30	0.66	1.30	0.04	22.11	0.18	1.10	54
	100	0.1	0.71	0.09	21.50	0.14	0.14	83
Day 16 (st. 088)	20	0.11	0.54	0.04	21.66	0.14	0.07	88
	40	0.08	0.63	0.07	21.15	0.04	0.32	67

Soluble (<200 kDa) Fe(III)-binding ligands concentrations ($[L]_{soluble}$) and the conditional stability constants of the soluble ligands with soluble iron ($\log K'_{soluble}$) from the vertical casts. The standard deviations (stdv) are calculated as indicated in the text. Differences between dissolved and soluble ligands ($[L]_{dissolved} - [L]_{soluble}$) and percentages of soluble relative to dissolved ligands ($[L]_{soluble}/[L]_{dissolved}$) are indicated at each sampling depth.

b.d. denotes below detection limit of technique. Statistical errors on differences between [dissolved-L] and [soluble-L] were calculated as: $\sqrt{(stdv[diss\text{-}L]^2 + stdv[sol\text{-}L]^2)}$. At the out-patch station, all values are b.d., while at the in-patch stations, the differences were quite large and well exceeding the overall statistical errors. In addition, analytical errors induced by using [Fe] in the estimation of [L] is 5–6% of [Fe] (Nishioka et al., in press). The resulting analytical errors introduced by iron measurements on the calculation of [dissolved-L] − [soluble-L] were calculated as $\sqrt{(stdv[diss\text{-}Fe]^2 + stdv[sol\text{-}Fe]^2)}$, and accounted for 3–27% of this difference (5–14% in the natural waters). This indicated that the analytical errors induced by iron measurements in the estimation of these differences were not significant.

ND denotes Not Determined (e.g., no mathematical resolution).

Depths in italic indicate high [DFe] (>1.7 nM).

Underlined depths indicate straight titrations in the dissolved fraction.

Next, after each storm event, the concentrations decreased in the mixed layer (Fig. 2), with a faster 5- to 7-fold decrease observed for the difference between dissolved and soluble ligands relative to an about 2-fold decrease of the soluble ligand pool (Fig. 2, Table 3);

ii) The proportion of soluble over dissolved ligands was modified after the first and second Fe-infusions compared to ambient waters (Table 3, Fig. 2). In the ambient waters (mean out-patch station), the size fractionation of the dissolved ligand was dominated by soluble ligands through the first top-100 m, with at least, $91 \pm 3\%$ of dissolved ligands concentration being smallest than 200 kDa (Table 3 and Fig. 2, and Boye et al., in prep.). In contrast, the soluble ligand was only about 55% of the dissolved ligand in the mixed layer after Fe-release (Table 3), leaving a significant portion of dissolved ligand (~45%) to exist as presumably colloidal ligand. After the storm, the later portion dropped faster than the [soluble-L] within the mixed layer, and thus soluble ligands once more dominated (by about 70–80%) the dissolved ligands pool (Fig. 2), yet never reaching the complete ~91% dominance of the unperturbed ambient waters of out-patch stations.

In deeper waters, below the mixed layer, insufficient data were available to draw definitive conclusions (Table 3). The only two stations sampled in deeper water after Fe-releases (Days 1 and 12) indicated that soluble ligands were predominant in deeper waters, either in the natural waters or after the first and the second Fe-additions (Figs. 1–2).

4. Discussion

4.1. Fe-speciation determinations

Associated with the exceptionally high (>1.7 nM) and persistent DFe in the mixed layer waters following the Fe-infusions, [DFe] most often exceeded the estimated dissolved-*L* concentrations (by 0.88 nM on average, $n=16$), unlike the natural, post-storms and in-patch deeper waters conditions (Fig. 1). Moreover, saturated linear titration curves were observed for discrete samples (underlined in Table 2) containing such high [DFe] indicating that the stronger Fe-binding complexes (e.g. with a higher $\alpha_{FeL}=K'_{FeL}[L]$ than a_{FeTAC2}) were already saturated with the infused iron before starting the titration. These both, in turn, make it difficult to estimate a reliable ligand Fe-binding capacity.

Furthermore, with regards to the sharp increase of the colloidal iron fraction following the Fe-infusions (Nishioka et al., in press), it is possible that the actual ligand Fe-binding capacity detected by the titrations was substantially influenced by inorganic colloids. For example, the infused Fe(II) which was still detectable for several days in the surface mixed layer (Croot et al., in press) would have been largely oxidized to Fe(III) under the titration conditions (e.g., long equilibration time at room temperature, without natural light) (Johnson et al., 1994; Stumm and Morgan, 1996). The colloidal Fe(III) oxyhydroxides, either formed in the titration-sample or already present in the infused waters, would thus rapidly precipitate under these conditions and possibly would form surface active amorphous colloids (Wells, 2003) that appeared as a (saturated) strong Fe-binding capacity upon titration (Croot and Johansson, 2000). Despite this possibility, there is evidence that at least some (53% on average) of the ligand Fe-binding capacity was soluble organic ligands. The detection of free soluble organic ligand by well-curved titrations associated with a significant excess of [soluble-*L*] over [soluble-Fe] during the high [DFe] periods (Fig. 1) indicated indeed the doubtless presence of soluble organic material in the dissolved pool. Overall, the actual ligand Fe-binding capacity detected by the titrations here could be a mixture of inorganic colloids and organic forms (colloidal and/or soluble) which formed a myriad of strong complexes with Fe. Whatever their chemical natures and their size-distribution and despite [DFe] exceeding [*L*], the ligands were obviously acting to sustain still large amounts of dissolved Fe in the infused mixed layer waters for several days, since [*L*] represented on average 75% of [DFe] in the mixed layer during the high-Fe periods (Fig. 1).

4.2. Vertical distribution and temporal changes of the ligand concentrations

4.2.1. The dynamics of the dissolved ligands

In surface waters within the mixed layer, the distribution of the dissolved ligand was strongly influenced by the physical transport processes, such as vertical dilution due to wind stress during and after storm events (Bakker et al., in press) and horizontal dispersion due to strong surface currents, as measured in the north-eastern part of the infused eddy after the first infusion (Strass et al., 2001). For example, dilution and diffusion of the patch with ambient natural waters, or from below the Fe-infused mixed layer containing lower ligand concentrations (~0.7–0.8 nM), could both account for the observed decrease of the ligand concentration in surface waters after storm events. Next to Fe-infusions, the distribution of the dissolved ligands in the fertilized mixed layer was strongly influenced by productive processes (chemical and/or biological), in addition with the physical dilution processes. For instance, the chemical reactions which formed colloidal Fe(III) oxyhydroxides in the Fe-infused waters and further formed surface active amorphous colloids (Wells, 2003) could partly account for the observed increase of [dissolved-*L*] (see above). In addition, the major biological response to the Fe-infusions was an induced bloom, with up to 4- to 6-fold increases in chlorophyll-*a* and in primary productivity (nano- and micro-phytoplankton) inside the patch as compared to outside the patch (Gervais et al., 2002). The first biological changes were seen in the photosynthetic efficiency of the phytoplankton (Gervais et al., 2002). This induced bloom may also have been a source of dissolved ligands. The overall pattern of the ligand increase reflecting of the increase of biomass (chl-*a*) after the first and second Fe-releases would indeed suggest a significant biological source of the ligands. This possibility was further supported by the good fit

of the maxima of [L] with [Chl-a] at almost the same depths:

$$[L]_{\mathrm{nmol/l}} = 1.70[\mathrm{Chl-a}]_{\mu\mathrm{g/l}} + 0.18 \ (R2 = 0.61 \text{ for } n = 39) \qquad (4)$$

for stations from Days 1 to 4 and Days 8 to 12. The biological source would include either (i) an active production, or (ii) an inadvertent release by recycling and regeneration of Particulate Organic Matter (POM), or (iii) a release by passive phytoplankton exudation. However, the Dissolved Organic Carbon (DOC) concentrations showed no systematic trends over the duration of the experiment (S. Gonzalez, personal communication), unlike the temporal changes observed for the ligands (Fig. 1). This contrast suggests that ligand production was probably decoupled from the major sources of DOC, such as bacterial recycling of the POM. Furthermore, the temporal changes of the ligand concentration after the third Fe-infusion (hardly any increase) were not well correlated with those of the Chl-a levels (still increased greatly up to ~6-fold relative to initial out-patch levels and by about 1.5× relative to pre-third infusion; Gervais et al., 2002) and neither with changes of the biogenic particles in the mixed layer (Gervais et al., 2002). These decouplings indicate that passive exudation would not be a likely source of the ligands. Instead the ligand production mediated by biological processes may have been regulated as an active functional response of the plankton community to an iron-release.

The dynamics of the ligands production as observed during EisenEx would only resemble the actively produced strong ligands class detected in IronEx-II (Rue and Bruland, 1997). In contrast, it did not mimic the passive production of the weaker ligands class, associated with recycling of organic biogenic material and phytoplanktonic cells leakages, detected in IronEx-II (Rue and Bruland, 1997). Moreover, it did not resemble the organic ligands observed at the end of the SOIREE survey, which had been ascribed to cell leakage and microzooplankton grazing of cells (Croot et al., 2001).

The lag-period observed between rapid increases of the ligands concentration in the mixed layer and the further slight increase in deeper waters below the mixed layer could be the result of a downward export of the ligands produced in surface waters. On the other hand, the slight increase of ligand concentrations in deeper waters during the experiment compared to dramatic changes observed in the mixed layer depth would indicate that overall the ligands did not strongly accumulate in deep waters (Fig. 2). The dilution processes would probably cause the relatively low export of the ligands, while it is also possible that the residence time of dissolved ligands was rather short in deep waters.

4.2.2. The size-distribution of the dissolved ligands

The soluble-L concentrations were lower than the dissolved-L concentrations, and the estimated stability constants of the soluble and dissolved ligands were in the same ranges ($\log K'_{\mathrm{dissolved}}$ and $\log K'_{\mathrm{soluble}}$ ~22), confirming the recovery of the soluble ligand in the determination of the dissolved ligand. It suggests also that the dissolved ligands encompassed several physico-chemical organic structures instead of being a single group of identical organic molecules. It is obvious in fact that more than two classes of organic ligands which were defined so far, either by chemical differences of abundance and binding strength with dissolved iron (such as in the Pacific Ocean, Rue and Bruland, 1995, 1997), or by physical differences (size fractions, Wu et al., 2001; and this study), co-occurred in the dissolved pool. Further studies are needed to better elucidate the distribution in size of dissolved ligands, as well as their chemical Fe-binding functions.

The trends observed for the discrete determinations of soluble ligands and of the difference between dissolved and soluble ligands (e.g., presumably colloidal ligands) in the mixed layer were fitting well with those of iron in each size fraction (see results section and Nishioka et al., in press). Furthermore, the apparent shift in the proportions of soluble ligands and of the difference between dissolved and soluble ligands induced by Fe-infusions was also consistent with the observations made during the IronEx-II experiment. Here a shift had taken place from predominance of soluble ligands (<1 kDa) in natural waters towards the colloidal fraction (>1 kDa–<0.4 μm) right after the first Fe-infusion (Rue and Bruland, 1997). The dynamics of the two size classes of ligands observed here suggested, in addition, that the colloidal fraction would be the most reactive size class, this

being the primarily produced ligand pool upon Fe-infusion as well as the most efficiently lost phase upon storm mixing and dilution. It has been argued that despite their expected small settling rates, the colloidal Fe species can aggregate in larger agglomerates, which next settle out into deeper oceanic waters, possibly acting as a major route of Fe-removal (Wu et al., 2001). Yet the major route of the preferential loss of the colloidal Fe species in the present study appeared to be linked with storm events. Thus superimposed on the general dilution of all substances due to storms, the scavenging processes onto biogenic particles enhanced by strong storm-induced mixing would specifically enhance the loss of the colloidal phase in this study.

4.3. Peculiar features and implications for the iron cycling

Unexpectedly [DFe] most often exceeded dissolved-[*L*] in the mixed layer of the Fe-infused waters (Figs. 1 and 3). While in itself these ligands are being produced rapidly and significantly, the production was indeed not sufficient or still too slow (compared to the sharp increase of [DFe] caused by Fe-releases) to exceed [DFe] and thus to ensure complete stabilization of the dissolved iron, by its complexation with strong dissolved Fe-binding ligands. This pattern differs greatly with the situation observed in natural oceanic waters (Rue and Bruland, 1995; Gledhill and van den Berg, 1994; Witter and Luther, 1998; Powell and Donat, 2001; Van den Berg, 1995; Witter et al., 2000; Boye et al., 2001), even in oceanic regions receiving greater Fe-inputs (Boye et al., 2003; Van den Berg, 1995; Wu and Luther, 1995). The developments observed during EisenEx indicate very peculiar features of Fe-speciation upon Fe-enrichment experiment in the Southern Ocean compared to ambient oceanic waters.

Associated with the general excess of [DFe] over dissolved-[*L*] in the infused mixed layer, a remaining significant portion of dissolved Fe (13–40%, Fig. 3) occurred uncomplexed by strong Fe(III)-binding ligands (those with a higher $\alpha_{FeL}=K'_{FeL}$ [*L*] than a_{FeTAC2}). This fraction ranged between ~0.2 and 2 nM, well above the iron solubility (0.1 nM; Wu et al., 2001). For instance [soluble-*L*] was in excess over [soluble-Fe] (by ~0.5 nM; Fig. 3) in the water column

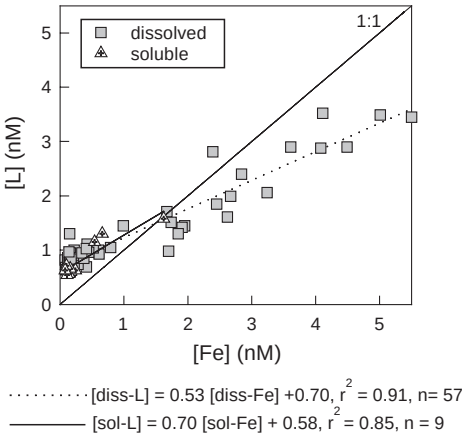

Fig. 3. Relationships between the concentration of the iron (horizontal axis) and the ligand concentration (vertical axis) in each size fraction: dissolved are filled squares, soluble are open triangles. Data are for the in-patch values obtained throughout the 0- to 100-m water column.

of the patch area, suggesting that soluble-Fe was primarily stabilized upon complexation with strong soluble ligands (up to 99.7%) at the thermodynamic equilibrium. In contrast, the difference between [dissolved-*L*] and [soluble-*L*] was generally lower than [colloidal-Fe] (equal to the difference between [dissolved Fe] and [soluble-Fe], Nishioka et al., in press) in the surface infused mixed layer, leaving a 10–76% portion of colloidal iron to exist in a weakly bound form, probably as inorganic colloids. The increase of [DFe] resulting principally from an increase of colloidal-Fe concentrations after Fe-infusion (Nishioka et al., in press) would further suggest that the fertilizer-Fe(II) was rapidly becoming converted into mainly colloids within the surface infused mixed layer, this also accounting for including the weakly bound dissolved Fe portion. The persistence of such high concentrations of weakly bound iron complexes, which probably occurred as inorganic colloids, above Fe-solubility limits, instead of a rather expected rapid loss due to colloids aggregation, would depict peculiar features of the chemical iron cycling here. Next to it persistent high dissolved iron concentrations were also observed in the infused waters (Nishioka et al., in press). Among the chemical features of the Fe cycling in these waters, the stability of high Fe(II) concentrations in the surface mixed layer of the EISENEX patch (Croot et al., in press) indicated that the thermodynamic

equilibrium was not reached in the infused waters. Chemical reactions between colloidal-Fe(III) and Fe(II) (Croot et al., in press; Rijkenberg et al., 2005) and key features of the Fe-redox cycling in these oceanic waters (Croot et al., 2001; Liu and Millero, 2002) would further explain the unexpected persistence of high concentrations of weakly bound dissolved iron, which in turn would promote an overall high [DFe] concentration to be sustained. Despite such features, dissolved iron, either strongly or weakly bound, was ultimately not prevented from being lost by dynamical processes (such as lateral and vertical mixing during storm events).

Acknowledgments

The authors are most grateful for the assistance and logistical support provided by the officers and crew of the R.V. Polarstern, the Chief Scientist Victor Smetacek (AWI), Uli Bathmann (AWI), and Andy Watson (U.K.) for their efforts. We thank Dr L. Gerringa (NIOZ) for her helpful comments on this paper. This work was financed by the European Community projects CARUSO (ENV4-CT97-0472) and IRONAGES (EVK2-CT1999-00031).

References

Bakker, D.C.E., Bozec, Y., Nightingale, P.D., Goldson, L., Messias, M.J., de Baar, H.J.W., Liddicoat, M., Skjelvan, I., Strass, V., Watson, A.J., in press. Iron and mixing affect biological carbon uptake in SOIREE and EisenEx, two Southern Ocean iron fertilisation experiments. Deep-Sea Research I.

Barbeau, K., Rue, E.L., Bruland, K.W., Butler, A., 2001. Photochemical cycling of iron in the surface ocean mediated by microbial iron(III)-binding ligands. Nature 413, 409–413.

Bowie, A.R., Maldonado, M.T., Frew, R.D., Croot, P.L., Achterberg, E.P., Mantoura, R.F.C., Worsfold, P.J., Law, C.S., Boyd, P.W., 2001. The fate of added iron during a mesoscale fertilization experiment in the Southern Ocean. Deep-Sea Research II 48, 2473–2703.

Boyd, P.W., Law, C.S., 2001. The Southern Ocean Iron RElease Experiment (SOIREE)—introduction and summary. Deep-Sea Research II 48, 2425–2438.

Boyd, P.W., Law, C.S., Wong, C.S., Nojiri, Y., Tsuda, A., Levasseur, M., Takeda, S., Rivkin, R., Harrison, P.J., Strzepek, R., Gower, J., McKay, R.M., Abraham, E., Arychuk, M., Barwell-Clarke, J., Crawford, W., Crawford, D., Hale, M., Harada, K., Johnson, K., Kiyosawa, H., Kudo, I., Marchetti, A., Miller, W., Needoba, J., Nishioka, J., Ogawa, H., Page, J., Robert, M., Saito, H., Sastri, A., Sherry, N., Soutar, T., Sutherland, N., Taira, Y., Whitney, F., Wong, S.K.E., Yoshimura, T., 2004. The decline and fate of an iron-induced subarctic phytoplankton bloom. Nature 428, 549–553.

Boye, M., van den Berg, C.M.G., 2000. Iron availability and the release of iron complexing ligands by *Emiliania huxleyi*. Marine Chemistry 70, 277–287.

Boye, M., van den Berg, C.M.G., de Jong, J.T.M., Leach, H., Croot, P.L., de Baar, H.J.W., 2001. Organic complexation of iron in the Southern Ocean. Deep Sea Research I 48, 1477–1497.

Boye, M., Aldrich, A.P., van den Berg, C.M.G., de Jong, J.T.M., Veldhuis, M., de Baar, H.J.W., 2003. Horizontal gradient of the chemical speciation of iron in surface waters of the northeast Atlantic Ocean. Marine Chemistry 80, 129–143.

Boye, M., Nishioka, J., Croot, P.L., Laan, P., Timmermans, K., Takeda, S., and de Baar, H.J.W., in preparation. Colloidal Fe accounts for a significant portion of dissolved organic Fe-complexes in the Southern Ocean.

Bozec, Y., Bakker, D.C.E., Hartmann, C., Thomas, H., Bellerby, R.G.J., Nightingale, P.D., Riebesell, U., Watson, A.J., de Baar, H.J.W., in press. The CO_2 system in a Redfield context during an iron enrichment experiment in the Southern Ocean. Marine Chemistry. Published online ahead of print December 8, 2004. doi:10.1016/j.marchem.2004.08.004.

Coale, K.H., Johnson, K.S., Fitzwater, S.E., Gordon, R.M., Tanner, S., Chavez, F.P., Ferioli, L., Sakamoto, C., Rogers, P., Millero, F., Steinberg, P., Nightingale, P., Coopr, D., Cochlan, W.P., Landry, M.R., Constantinou, J., Rollwagen, G., Trasvina, A., Kudela, R., 1996. A massive phytoplankton bloom induced by an ecosystem-scale iron fertilization experiment in the equatorial Pacific Ocean. Nature 383, 495–501.

Coale, K.H., et al., 2004. Southern ocean iron enrichment experiment: carbon cycling in high- and low-Si waters. Science 304, 408–414.

Croot, P.L., Johansson, M., 2000. Determination of iron speciation by cathodic stripping voltammetry in seawater using the competing ligand 2-(2-Thiazolylazo)-p-cresol (TAC). Electroanalysis 12 (8), 565–576.

Croot, P.L., Bowie, A.R., Frew, R.D., Maldonado, M.T., Hall, J.A., Safi, K.A., LaRoche, J., Boyd, P.W., Law, C.S., 2001. Retention of dissolved iron and Fe^{II} in an iron induced Southern Ocean phytoplankton bloom. Geophysical Research Letters 28, 3425–3428.

Croot, P.L., Anderson, K., Oztürk, M., Turner, D.R., 2004. The distribution and speciation of iron along 6°E in the Southern Ocean. Deep-Sea Research II 51, 2857–2879.

Croot, P.L., Laan, P., Nishioka, J., Strass, V., Cisewski, B., Boye, M., Timmermans, K.R., Bellerby, R.G., Goldson, L., Nightingale, P., de Baar, H.J.W., in press. Spatial and Temporal distribution of Fe(II) and H_2O_2 during EisenEx, an open ocean mescoscale iron enrichment. Marine Chemistry. Published online ahead of print February 19, 2005. doi:10.1016/j.marchem.2004.06.041.

Gervais, F., Riebesell, U., Gorbunov, M.Y., 2002. Changes in primary productivity and chlorophyll a in response to iron fertilization in the Southern Polar Frontal Zone. Limnology and Oceanography 47 (5), 1324–1335.

Gledhill, M., van den Berg, C.M.G., 1994. Determination of complexation of iron(III) with natural organic complexing ligands in sea water using cathodic stripping voltammetry. Marine Chemistry 47, 41–54.

Goldson, L., in press. Vertical mixing across the seasonal pycnocline of the Southern Ocean: Studies using sulphur hexafluoride tracer. PhD thesis, University of East Anglia, Norwich, U.K, 219 pp.

Gordon, R.M., Johnson, K.S., Coale, K.H., 1998. The behaviour of iron and other trace elements during the IronEx-I and PlumEx experiments in the Equatorial Pacific. Deep-Sea Research II 45, 995–1041.

Hudson, R.J.M., Covault, D.T., Morel, F.M.M., 1992. Investigations of iron coordination and redox reactions in seawater using ^{59}Fe radiometry and ion-pair solvent extraction of amphiphilic iron complexes. Marine Chemistry 38, 209–235.

Hunter, K.A., Boyd, P.W., Bruland, K.W., Buffle, J., Buat-Ménard, P., de Baar, H.J.W., Duce, R.A., Sunda, W.J., Jickells, T.D., Moffet, J.W., Rue, E.L., Spokes, L.J., Sulzberger, B., Turner, D.R., Waite, T.D., Watson, A.J., Whitfield, M., 2001. The Biogeochemistry of Iron in Seawater, Summary and Recommendations. Wiley, Chichester, pp. 123–253.

Johnson, K.S., Coale, K.H., Elrod, V.A., Tindale, N.W., 1994. Iron photochemistry in waters from the equatorial Pacific Ocean. Marine Chemistry 46, 319–334.

Kuma, K., Nishioka, J., Matsunaga, K., 1996. Controls on iron(III) hydroxide solubility in seawater: the influence of pH and natural organic chelators. Limnology and Oceanography 41, 396–407.

Liu, X., Millero, F.J., 2002. The solubility of iron in seawater. Marine Chemistry 77, 43–54.

Martin, J.H., Coale, K.H., Johnson, K.S., Fitzwater, S.E., Gordon, R.M., Tanner, S.J., Hunter, C.N., Elrod, V.A., Nowicki, J.L., Coley, T.L., Barber, R.T., Lindley, S., Watson, A.J., van Scoy, K., Law, C.S., Liddicoat, M.I., Ling, R., Station, T., Stockel, J., Collins, C., Anderson, A., Bidigare, R., Ondrusek, M., Latasa, M., Millero, F.J., Lee, K., Yao, W., Zhang, J.Z., Friederich, G., Sakamoto, C., Chavez, F., Buck, K., Kolber, Z., Green, R., Falkowski, P., Chisholm, S.W., Hoge, F., Swift, R., Yangel, J., Turner, S., Nightingale, P., Hatton, A., Liss, P., Tindale, N.W., 1994. Testing the iron hypothesis in ecosystems of the equatorial Pacific Ocean. Nature 371, 123–129.

Nishioka, J., Takeda, S., Wong, C.S., Johnson, W.K., 2001. Size-fractionated iron concentrations in the northeast Pacific Ocean: distribution of soluble and small colloidal iron. Marine Chemistry 74, 157–179.

Nishioka, J., Takeda, S., de Baar, H.J.W., Croot, P.L., Boye, M., Laan, P., Timmermans, K.R., in press. Changes in the concentration of iron in different size fractions during an iron enrichment experiment in the open Southern Ocean. Marine Chemistry. Published online ahead of print December 30, 2004. doi:10.1016/j.marchem.2004.06.040.

Obata, H., Karatani, H., Nakayama, E., 1993. Automated determination of iron in seawater by chelating resin concentration and chemiluminescence detection. Analytical Chemistry 65, 1524–1528.

Powell, R.T., Donat, J.R., 2001. Distributions of organic Fe complexing ligands in the South and Equatorial Atlantic. Deep-Sea Research-II 48 (13), 2877–2893.

Reid, R.T., Butler, A., 1991. Investigation of the mechanism of iron acquisition by the marine bacterium *Alteromonas luteoviolaceus*: characterization of siderophore production. Limnology and Oceanography 36, 1783–1792.

Reid, R.T., Live, D.G., Faulkner, D.J., Butler, A., 1993. A siderophore from a marine bacterium with an exceptional ferric ion affinity constant. Nature 366, 455–458.

Rijkenberg, M.J.A., Fischer, A.C., Kroon, J.J., Gerringa, L.J.A., Timmermans, K.R., Wolterbeek, H.T., de Baar, H.J.W., 2005. The influence of UV irradiation on the photoreduction of iron in the Southern Ocean. Marine Chemistry 93, 119–129.

Rue, E.L., Bruland, K.W., 1995. Complexation of iron (III) by natural organic ligands in the Central North Pacific as determined by a new competitive ligand equilibration/adsorptive cathodic stripping voltammetric method. Marine Chemistry 50, 117–138.

Rue, E.L., Bruland, K.W., 1997. The role of organic complexation on ambient iron chemistry in the equatorial Pacific Ocean and the response of a mesoscale iron addition experiment. Limnology and Oceanography 42 (5), 901–910.

Ruzic, I., 1982. Theoretical aspects of the direct titration of natural waters and its information yield for trace metal speciation. Analytica Chimica Acta 140, 99–113.

Strass, V.H., et al., 2001. The physical setting of the Southern Ocean iron fertilisation experiment. Berichte zur Polar-und Meeresforschung 400, 94–130.

Stumm, W., Morgan, J.J., 1996. Aquatic chemistry, Third edition, Wiley-Interscience Publication John Wiley and Sons, Inc., 1022.

Tsuda, A., Takeda, S., Saito, H., Nishioka, J., Nojiri, Y., Kudo, I., Kiyosawa, H., Shiomoto, A., Imai, I., Ono, T., Shimamoto, A., Tsumune, D., Yoshimura, T., Aono, T., Hinuma, A., Kinugasa, M., Suzuki, K., Sohrin, Y., Noiri, Y., Tani, H., Deguchi, D., Tsurushima, N., Ogawa, H., Kukami, K., Kuma, K., Saino, T., 2003. A mesoscale iron enrichment in the western subartic Pacific induces large centric diatom bloom. Science 300, 958–961.

van den Berg, C.M.G., 1982. Determination of copper complexation with natural organic ligands in seawater by equilibration with MnO_2. Marine Chemistry 11, 307–322.

van den Berg, C.M.G., 1995. Evidence for organic complexation of iron in seawater. Marine Chemistry 50, 139–157.

van den Berg, C.M.G., Donat, J.R., 1992. Determination and data evaluation of copper complexation by organic ligands in sea water using cathodic stripping voltammetry at varying detection windows. Analytica Chimica Acta 257, 281–291.

van den Berg, C.M.G., Kramer, J.R., 1979. Determination of complexing capacities and conditional stability constants for copper in natural waters using MnO_2. Analytica Chimica Acta 106, 113–120.

Wells, M.L., 2003. The level of iron enrichment required to initiate diatom blooms in HNLC waters. Marine Chemistry 82, 101–114.

Wells, M.L., Kozelka, P.B., Bruland, K.W., 1998. The complexation of 'dissolved' Cu, Zn, Cd and Pb by soluble and colloidal organic matter in Narragansett Bay, R.I. Marine Chemistry 62, 203–217.

Witter, A.E., Luther III, G.W., 1998. Variation in Fe-organic complexation with depth in the Northwestern Atlantic Ocean as determined using a kinetic approach. Marine Chemistry 62, 241–258.

Witter, A.E., Lewis, B.L., Luther III, G.W., 2000. Iron speciation in the Arabian Sea. Deep Sea Research II 47, 1517–1539.

Wu, J.F., Luther III, G.W., 1995. Complexation of Fe(III) by natural organic ligands in the Northwest Atlantic Ocean by competitive ligand equilibration method and a kinetic approach. Marine Chemistry 50, 159–178.

Wu, J.F., Boyle, E., Sunda, W., Wen, L.S., 2001. Soluble and colloidal iron in the oligotrophic North Atlantic and North Pacific. Science 293 (5531), 847–849.